Acta Biochim Biophys Sin 2023, 55(4): 613–622
https://doi.org/10.3724/abbs.2023050
Advance Access Publication Date: 28 March 2023
Original Article

Original Article

Glutathione disrupts galectin-10 Charcot-Leyden crystal formation to possibly ameliorate eosinophil-based diseases such as asthma

Heya Na[1,†], Hend Sayed[1,†], Gabriela Jaramillo Ayala[1], Xing Wang[1], Yuhan Liu[1], Jinyi Yu[1], Tianhao Liu[1], Kevin H. Mayo[2], and Jiyong Su[1,*]

[1]Engineering Research Center of Glycoconjugates Ministry of Education, Jilin Provincial Key Laboratory of Chemistry and Biology of Changbai Mountain Natural Drugs, School of Life Sciences, Northeast Normal University, Changchun 130024, China, and [2]Department of Biochemistry, Molecular Biology & Biophysics, 6-155 Jackson Hall, University of Minnesota, 321 Church Street, Minneapolis, Minnesota 55455, USA
[†]These authors contributed equally to this work.
*Correspondence address. +86-431-85099350; E-mail: sujy100@nenu.edu.cn

Received 15 September 2022 Accepted 23 November 2022

Abstract

Charcot-Leyden crystals (CLCs) are the hallmark of many eosinophilic-based diseases, such as asthma. Here, we report that reduced glutathione (GSH) disrupts CLCs and inhibits crystallization of human galectin-10 (Gal-10). GSH has no effect on CLCs from monkeys (*Macaca fascicularis* or *M. mulatta*), even though monkey Gal-10s contain Cys29 and Cys32. Interestingly, human Gal-10 contains another cysteine residue (Cys57). Because GSH cannot disrupt CLCs formed by the human Gal-10 variant C57A or inhibit its crystallization, the effects of GSH on human Gal-10 or CLCs most likely occur by chemical modification of Cys57. We further report the crystal structures of Gal-10 from *M. fascicularis* and *M. mulatta*, along with their ability to bind to lactose and inhibit erythrocyte agglutination. Structural comparison with human Gal-10 shows that Cys57 and Gln75 within the ligand binding site are responsible for the loss of lactose binding. Pull-down experiments and mass spectrometry show that human Gal-10 interacts with tubulin α-1B, with GSH, GTP and Mg^{2+} stabilizing this interaction and colchicine inhibiting it. Overall, this study enhances our understanding of Gal-10 function and CLC formation and suggests that GSH may be used as a pharmaceutical agent to ameliorate CLC-induced diseases.

Key words asthma, Charcot-Leyden crystal, glutathione, galectin-10, tubulin α-1B

Introduction

In 1853 and 1872, Jean-Martin Charcot and Ernst Viktor von Leyden discovered the existence of hexagonal and bipyramidal Charcot-Leyden crystals (CLCs) in spleen-rich eosinophils and in the sputum of patients with bronchial asthma, respectively [1,2]. The primary and tertiary structures of CLC protein are highly conserved [3–5] to other galectins, and therefore referred to as galectin-10 (Gal-10) [6]. Gal-10 is overexpressed in eosinophils [7] and can spontaneously form CLCs within these cells [8] or upon eosinophil lysis [9]. CLCs are frequently observed in eosinophil-based diseases, such as acute myeloid leukemia, mastocytoma [10], allergic rhinitis [11], celiac disease [12], and eosinophilic cystitis [13]. Recently, a humanized mouse model was used to demonstrate that CLCs directly induce asthma [14]. Anti-Gal-10 antibodies can rapidly dissolve or disrupt CLCs and reverse the symptoms caused by CLCs in the airway [14]. However, numerous reports indicate that Gal-10 does not always form CLCs [15–17], suggesting that some as yet-unknown compound(s) can inhibit Gal-10 crystallization and keep Gal-10 in solution. These compound(s) may potentially be used as pharmaceutical agents against CLC/eosinophil-based diseases, such as asthma. Here, we identified a few compounds that achieve this goal.

Gal-10 is a prototype galectin [18–20], and natural or recombinant human Gal-10 readily crystallizes to form CLCs [21–26]. Our previous studies demonstrated that two Gal-10 monomers form a homodimer via interactions between the S-faces of their carbohydrate recognition domains (CRDs) [25,26]. In this regard, the global form of Gal-10 is significantly different from that of other prototype galectins, including Gal-1 [27], Gal-2 [28], Gal-7 [29], Gal-13

[30–32], Gal-14 [33], and Gal-16 [33,34]. In human Gal-10 dimers, a key tyrosine residue (Tyr69) from one monomer subunit interacts with Tyr69 from the other subunit via aromatic-ring stacking, an interaction that drives Gal-10 crystallization [14]. Antibodies targeting the epitope around Tyr69 can dissolve/disrupt CLCs by abolishing this aromatic-ring-stacking interaction [14]. However, even though tyrosine is replaced by phenylalanine in Gal-10 from other primates (such as *Macaca fascicularis* and *M. mulatta*), it is unknown whether this substitution affects Gal-10 dimerization and CLC formation.

In human galectins (*e.g.*, Gal-1, Gal-3, and Gal-8), there are several highly conserved residues within the canonical CRD-ligand-binding site [25,35] to which β-galactosides (such as lactose) bind. Compared to other galectins, human Gal-10 contains several amino acid substitutions in its ligand binding site [25,35] that inhibit Gal-10 binding to lactose [22,25,26]. Nevertheless, when CLCs are soaked in high concentrations (~50% saturation) of various monosaccharides, Gal-10 cocrystallizes with them [14,24], albeit with low affinity. A BLAST comparison of the primary structures of human and other primate Gal-10s (https://blast.ncbi.nlm.nih.gov/Blast.cgi) suggests that some primate Gal-10s may indeed be able to bind to lactose.

Gal-10 can be found in cells within the nucleus [16,25,26], granules [10], cytoplasm [17,36], outer-cell membrane [37] and inner-cell membranes [38]. This suggests that there could be several partners to which Gal-10 can bind and regulate distribution and/or transport through cell membranes, as well as possibly regulating the function of these partners. To date, only two enzymes (*i.e.*, lysophospholipase [23] and RNases [39]) are known to bind to Gal-10. However, there are likely other Gal-10 partners that remain unidentified.

In the present study, we screened several compounds for their ability to dissolve or disrupt CLCs and/or to inhibit Gal-10 crystallization. Our results showed that reduced glutathione (GSH) can function in this way. We also solved the crystal structures of Gal-10 from two monkeys (*M. fascicularis* and *M. mulatta*) that cocrystallized with lactose. In both monkey Gal-10s, phenylalanine replaces Tyr69, which promotes Gal-10 crystallization. Pull-down experiments and mass spectrometry show that Gal-10 binds to tubulin α-1B. Overall, our study reveals new structural features and functions of Gal-10.

Materials and Methods

Cloning, protein expression, and purification

The genes for *M. fascicularis* and *M. mulatta* Gal-10s were synthesized by SynBio Technologies (Monmouth Junction, USA) and cloned into pET28a vectors (Novagen, Gibbstown, USA). All constructs were transformed into *E. coli* BL21 (DE3) cells and plated onto LB agar plates supplemented with 100 μg/mL kanamycin. Following overnight culturing, *E. coli* BL21 (DE3) cells were scraped from the agar plates and transferred into 10 mL of LB medium containing 100 μg/mL kanamycin. This culture was then shaken at 37°C overnight. The following day, the LB medium containing *E. coli* BL21 (DE3) cells was transferred into 1 L of LB medium and shaken at 37°C. When the optical density of the cultures reached 0.6–1.2, IPTG (final concentration of 0.5 mM) was added to induce protein overexpression.

After overnight induction at 25°C, cells were harvested by centrifugation (6000 *g* for 15 min) and lysed by sonication in lysis buffer that consisted of 10 mM Tris/HCl, pH 8.0, 150 mM NaCl, 2 mM β-mercaptoethanol, and 20 mM imidazole. The protein from the clarified cell extract was purified using a Ni-NTA agarose column (Qiagen, Hilden, Germany). After purification, the His-tagged protein was dialyzed against 10 mM Tris/HCl, pH 8.0, 300 mM NaCl, and 2 mM β-mercaptoethanol, with thrombin (5 NIH units per milligram of protein) added to remove the His tag. SDS-PAGE demonstrated that the protein purity was >90%. Proteins were concentrated to approximately 2 mg/mL and stored at −80°C. Purification of human Gal-10 and two variants (C29A and C57A) was performed according to published protocols [25,26].

Crystallization, data collection, and structure determination

Crystals of *M. fascicularis* and *M. mulatta* Gal-10 were obtained after 7 and 10 days from hanging drops that contained 1 μL of 2 μg/μL protein and 1 μL solution containing 2 M imidazole (for *M. fascicularis* Gal-10) or 0.8 M imidazole (for *M. mulatta* Gal-10), pH 7.0, at room temperature. Prior to X-ray data collection, crystals of *M. fascicularis* and *M. mulatta* Gal-10 were soaked for approximately 4 min in a reservoir solution supplemented with 20% (w/v) PEG400, 20% (w/v) PEG400 and 10 mM lactose or 20% (w/v) glycerol. Crystals were flash cooled in liquid nitrogen, and datasets were collected at 100 K at the Shanghai Synchrotron Radiation Facility (Shanghai, China).

The datasets were indexed and integrated using the program XDS [40,41] and scaled using Aimless [42] from the CCP4 software package [43]. Structures were determined using Phaser [44] and molecular replacement with the structure of human Gal-10 (PDB: 5XRG) as the search model. Structure refinement and water updating were performed using Phenix [45] refinement and manual adjustment. Final structure validations were performed using MolProbity [46,47], and figures of all structures were generated using Chimera [48] and PyMOL (https://pymol.org/2/).

Hemagglutination assay

Chicken erythrocytes were prepared as described previously [25,26]. The hemagglutination assay was performed in microtiter V plates, with each well containing Gal-10s in 75 μL Tris buffer (10 mM Tris-HCl, 150 mM NaCl, pH 7.5) or 75 μL Tris buffer and 25 μL 4% (v/v) chicken erythrocyte suspensions. Cells were added, followed by shaking. Agglutination was allowed to proceed for 60 min on ice to ensure a consistent temperature. Lactose was used to inhibit the activity of Gal-10s.

Pull-down experiments and mass spectrometry

Prior to pull-down experiments, HeLa cells were cultured in RPMI 1640 growth medium supplemented with 10% newborn bovine serum and 100 units/mL penicillin-streptomycin at 37°C in an atmosphere of 5% CO_2/air. When the cell density reached approximately 80%, HeLa cells were scraped from the plate and treated with cell lysis buffer (50 mM Tris/acetate, pH 7.4, 0.5% Triton X-100, 150 mM NaCl, and 0.1 mM PMSF) for 30 min on ice and then centrifuged at 13,000 *g* for 15 min at 4°C. For pull-down experiments, 50 μg of His-tagged Gal-10 and 50 μg of HeLa cell lysate were incubated with 30 μL of Ni-NTA beads for 3 h at 4°C with constant agitation by rotation. Then, Ni-NTA beads were washed three times with PBS (136.8 mM NaCl, 2.7 mM KCl, 1 mM $Na_2HPO_4 \cdot 12H_2O$, and 0.18 mM KH_2PO_4, pH 7.2), supplemented

with 20 mM imidazole. The beads were collected and subsequently eluted with PBS, pH 7.2, supplemented with 500 mM imidazole. The eluted supernatant was collected and boiled in SDS-PAGE sample buffer and analyzed by SDS-PAGE. Protein bands were stained with Coomassie Brilliant Blue R-250 reagent. A protein band, which was specifically recovered with His-tagged Gal-10, was cut from SDS-PAGE and subjected to mass spectrometry analysis at Suzhou ProtTech Biopharmaceutical Company (Suzhou, China).

Western blot analysis

The pull-down procedures were the same as those described above. The supernatant was analyzed by SDS-PAGE and transferred onto PVDF membranes. The membranes were then blocked with 5% nonfat dry milk in 1 × PBST (PBS containing 0.05% Tween-20) for 1 h and incubated with anti-tubulin α-1B monoclonal antibody (1:3000, D191049; Sangon Biotech, Shanghai, China) overnight at 4° C, followed by incubation with HRP-conjugated goat anti-mouse IgG (1:5000, 3585047; Nachuan Biotech, Changchun, China) after three times wash with 1 × PBST. All protein blots were developed using an ECL Western Blotting Detection kit (Tanon™ ECL, 180–5001; Tanon, Shanghai, China). The effects of various compounds on the binding between Gal-10 and tubulin α-1B were also examined.

Determination of various compounds on CLC formation and dissolution.

Gal-10 could be crystallized in hanging drops that contained 1.8 μL of 1 μg/μL protein and 0.2 μL 50% (w/v) PEG-3350 at room temperature. To evaluate the effects of compounds on CLC formation, Gal-10 was incubated with 96 molecules from an additive screen (Hampton research) and several common compounds found in the lab for 5 min prior to the addition of PEG-3350. Then, the drops were equilibrated against 500 mL PBS, pH 7.2, contained in the reservoir wells. Following overnight incubation, the presence or absence of CLCs was evaluated with a microscope.

To evaluate the potency of various compounds to solubilize CLCs, CLCs were transferred from the hanging drops mentioned above into 1.8 μL PBS, pH 7.2. Then, 0.2 μL of various compounds was added to the drops. The drops were also equilibrated against 500 ml PBS, pH 7.2, contained in the reservoir wells. The effects of various compounds on the dissolution of CLCs were recorded with a camera under a microscope.

Results

Crystal structures of *M. fascicularis* and *M. mulatta* Gal-10

Following purification of Gal-10 from *M. fascicularis* and *M. mulatta*, we set up crystallization screens with both proteins. As with human Gal-10 [21–26], both monkey Gal-10s could be crystallized under different conditions, crystallizing as hexagonal bipyramidal crystals whose form is similar to that found in human Charcot-Leyden crystals (Figure 1A–C). Here, we solved their apo and lactose-bound structures by X-ray crystallography (Figure 1D–F).

Both monkey Gal-10 molecules crystallized as dimers, with

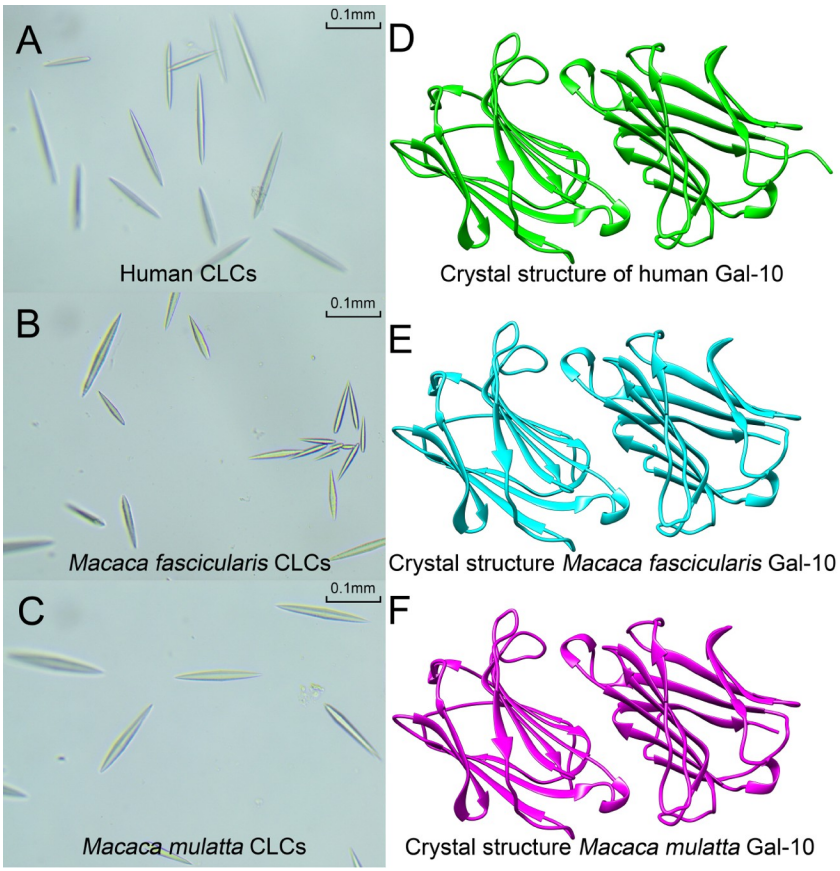

Figure 1. CLCs and crystal structures of Gal-10s (A–C) CLCs from humans, *Macaca fascicularis* and *Macaca mulatta*. All CLCs have hexagonal and bipyramidal forms. (D–F) Crystal structures of human Gal-10, *Macaca fascicularis* Gal-10 and *Macaca mulatta* Gal-10. All these Gal-10s crystallized as dimers.

similar global folds to human Gal-10 (Figure 1D–F), each forming dimers via interactions between their CRD S-faces. Gel filtration (Supplementary Figure S1) showed that the hydrodynamic sizes of all three Gal-10s were essentially the same, with the peak for human Gal-10 eluting at 12.16 mL and those of *M. fascicularis* and *M. mulatta* Gal-10 eluting at 11.41 mL and 11.61 mL, respectively (Supplementary Figure S1). The molecular weights of human, *M. fascicularis* and *M. mulatta* Gal-10s were calculated to be 25.4 kDa, 31.6 kDa and 29.8 kDa, respectively. In all instances, these molecular weights indicate the formation of dimers.

Crystal structure parameters for the two monkey Gal-10s are provided in Supplementary Table S1 and are highly similar to those for human Gal-10 [14]. Monomers of Gal-10 from *M. fascicularis* and *M. mulatta* contain the same number of β-strands as human Gal-10, with six β-strands (S1–S6) forming the sugar binding S-face and five β-strands (F1–F5) forming the opposing F-face (Figure 2) in the β-sandwich fold of their CRDs. Compared to human Gal-10 (PDB: 5XRH), differences in Cα root-mean-square deviations (RMSDs) are less than 2 Å, indicating that the global structures of monkey Gal-10s are similar to that of human Gal-10 (Figure 2, overlay figure). In terms of appearance and crystal-structure parameters, crystals of both monkey Gal-10s are Charcot-Leyden crystals, indicating that *M. fascicularis* and *M. mulatta* are suitable animal models to investigate Gal-10 as a pharmacological target for CLC-based diseases, such as asthma.

Ligand binding sites of Gal-10 from *M. fascicularis* and *M. mulatta*

We and other groups were not able to cocrystallize human Gal-10 with lactose, even when CLCs were soaked in relatively low concentrations of lactose or CLCs were grown from a buffer containing lactose [22,25,26]. However, Gal-10 could be cocrystallized with several monosaccharides when crystals were soaked in high concentrations of these sugars [22,14,24]. Here, we soaked *M. fascicularis* and *M. mulatta* CLCs in a buffer containing 10 mM lactose prior to freezing crystals in liquid nitrogen. After we collected the X-ray diffraction data, we solved the structures and could clearly observe lactose bound to both monkey-derived Gal-10s (Supplementary Figure S2).

To assess why human Gal-10 cannot bind to lactose, we compared its ligand binding site with those of the two monkey Gal-10s, along with those of human Gal-3 and Gal-8 N (Figure 3A). In the ligand binding sites of these galectins, there are six conserved residues. In all of these galectins, His53, Asn65 and Trp72 have analogous positions. However, compared to the other galectins,

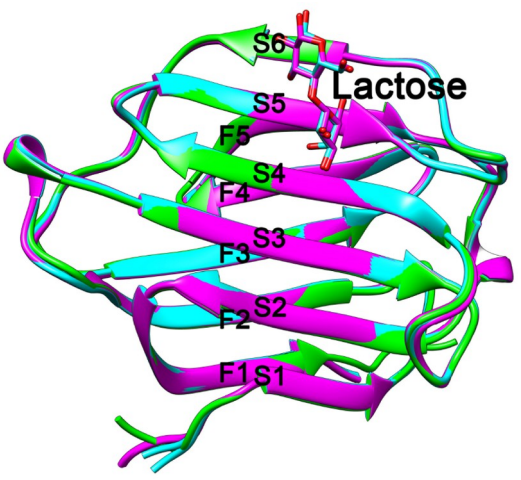

Figure 2. Overlay of human Gal-10 (green), *Macaca fascicularis* Gal-10 (cyan) and *Macaca mulatta* Gal-10 (purple) Three Gal-10s have similar structures. All of them have six and five β-strands at their CRD S- and F-faces, respectively. *Macaca fascicularis* Gal-10 and *Macaca mulatta* Gal-10 could be cocrystallized with lactose, but human Gal-10 could not.

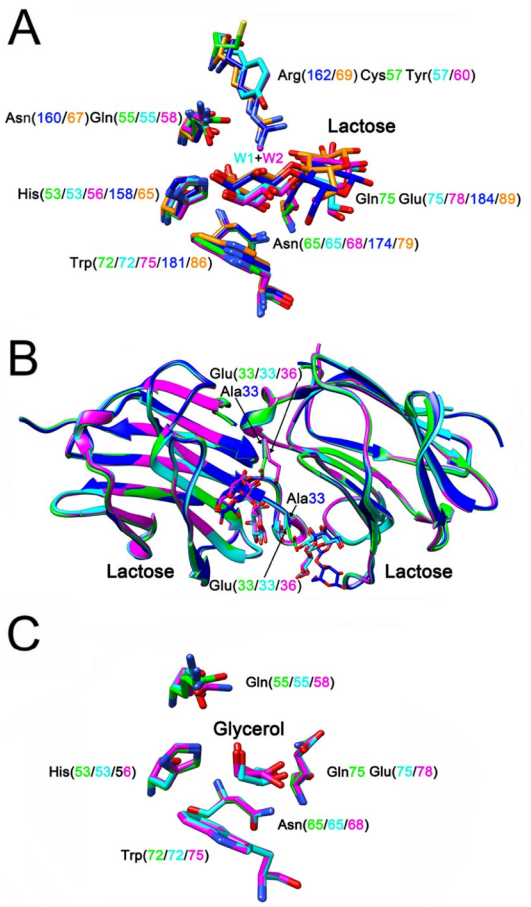

Figure 3. The ligand binding sites of Gal-10s (A) Comparison of ligand binding sites of human Gal-10 (green), *Macaca fascicularis* Gal-10 (cyan) and *Macaca mulatta* Gal-10 (purple) with Gal-3 (PDB: 4R9C, blue) [50] and Gal-8 N-terminal CRD (PDB: 5GZD, gold) [51]. Except human Gal-10, all other four galectins could bind to lactose. There are six conserved residues in the ligand binding site of these galectins. Human Gal-10 has a cysteine residue at position 57, while *Macaca fascicularis* Gal-10, *Macaca mulatta* Gal-10, Gal-3 and Gal-8 N-terminal CRDs have tyrosine and arginine residues at the same position. In addition, there is a glutamine residue at position 75 of human Gal-10, but all other galectins have a glutamate at the same position. Because of these two variations, human Gal-10 could not bind to lactose. The tyrosine residues of *Macaca fascicularis* Gal-10 and *Macaca mulatta* Gal-10 could indirectly stabilize lactose through a water molecule (W1 and W2, respectively). (B) The function of a glutamate residue outside the ligand binding site. The side chain of human Gal-10 Glu33 could directly reach the ligand binding site of another monomer. Therefore, Glu33 influences the interaction of human Gal-10 with lactose. The mutation of Glu33 to alanine could recover human Gal-10 binding to lactose [26]. In contrast, lactose bound to *Macaca fascicularis* Gal-10 and *Macaca mulatta* Gal-10 could directly influence the conformation of the glutamate residues (Glu33 and Glu36, respectively). (C) Human Gal-10 (green), *Macaca fascicularis* Gal-10 (cyan) and *Macaca mulatta* Gal-10 (purple) could bind to glycerol.

human Gal-10 has several differences involving residues Gln55, Cys57 and Gln75. Gln55 in human Gal-10 is replaced by either glutamine or asparagine in the other galectins. Nevertheless, changes from glutamine to asparagine and *vice versa* should not affect lactose binding. In human Gal-10, position 57 is a cysteine, whereas in *M. fascicularis* and *M. mulatta* Gal-10, there is a tyrosine (Tyr57 and Tyr60, respectively), and in Gal-3 and Gal-8 N, there are arginine residues (Arg162 and Arg68, respectively). Nevertheless, only human Gal-10 does not bind to lactose. Because Cys57 in human Gal-10 has a shorter side chain than tyrosine or arginine and its sulfhydryl group is not oriented toward the lactose binding site, Cys57 cannot coordinate with lactose, thus resulting in loss of lactose binding in human Gal-10.

In addition, Gal-3 Arg162 and Gal-8 Arg69 directly interact with lactose through their guanidine side chains. In contrast, Tyr57 in *M. fascicularis* Gal-10 and Tyr60 in *M. mulatta* Gal-10 can indirectly stabilize lactose via a water bridge (W1 and W2 in *M. fascicularis* and *M. mulatta* Gal-10, respectively), based on our previous study with Gal-13 variants in which a water molecule could mediate interactions between arginine and lactose [49]. In human Gal-10, there is a glutamine at position 75 (Gln75), whereas in the other four galectins, there is glutamate. Gln75 at this position may also decrease the ability of human Gal-10 to bind to lactose.

Because ligand binding sites in Gal-10 monomers face each other in the dimer state, the side chain of Glu33 from one monomer directly reaches the ligand binding site of the other monomer, thus affecting lactose binding. In a mutagenesis study with human Gal-10, we found that the E33A mutant could bind to lactose [26]. Because alanine has a shorter side chain than glutamate, it apparently does not enter the lactose binding space (Figure 3B). Both monkey Gal-10s have glutamate residues (Glu33 and Glu36) at the same position as human Glu33, yet lactose can still bind stably to these two monkey-derived Gal-10s (Supplementary Table S1). In both instances, lactose binding distorts the conformation of the glutamate (Figure 3B), indicating that this must be an optimal orientation of this residue for Gal-10 to bind to lactose. As with human Gal-10, both *M. fascicularis* and *M. mulatta* Gal-10 can be cocrystallized with glycerol (Figure 3C), which adopts a similar conformation to part of the galactose ring in lactose. Therefore, many galectins [25,30,50,51] bind to glycerol when used as a cryoprotectant.

Because *M. fascicularis* and *M. mulatta* Gal-10 can bind to lactose, we performed hemagglutination assay using chicken erythrocytes to evaluate the inhibitory effects (MIC values) of lactose on the two monkey Gal-10s. Human Gal-10 induces agglutination with a minimum agglutination concentration (MAC) of 3.1 μg/mL, consistent with previous results [25]. Whereas the MAC value for *M. fascicularis* Gal-10 is the same as that for human Gal-10, the MAC value for *M. mulatta* Gal-10 is much lower at 1.562 μg/mL (Figure 4). In addition, whereas human Gal-10 hemagglutination could not be inhibited by lactose [25], lactose inhibits hemagglutination mediated by both *M. fascicularis* and *M. mulatta* Gal-10s with MIC values of 12.5 mM and 6.25 mM, respectively (Figure 4). In these experiments, we used human Gal-10 and sucrose as negative controls.

Reduced glutathione dissolves CLCs and inhibits Gal-10 crystallization.

Anti-Gal-10 antibodies that block the dimer interface at Tyr69 in the Gal-10 CRD rapidly dissolve or disrupt CLCs in < 90 min and reverse asthmatic symptoms induced by CLCs [14]. Therefore, we hypothesized that small compounds that can bind to Gal-10 to disrupt dimer formation may also dissolve/disrupt CLCs and be more effective in treating eosinophil-based diseases caused by CLCs. Here, we investigated the use of small molecules to assess whether they could disrupt CLCs and inhibit Gal-10 crystallization.

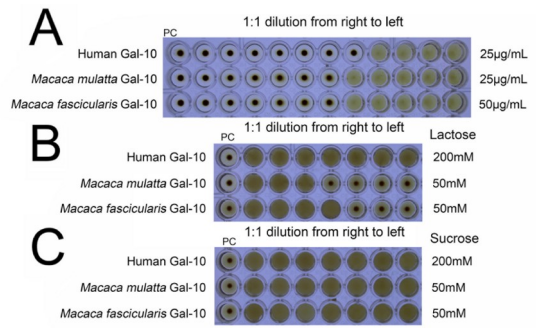

Figure 4. Hemagglutination assay with human Gal-10, *Macaca fascicularis* Gal-10 and *Macaca mulatta* Gal-10 (A) Human Gal-10, *Macaca fascicularis* Gal-10 and *Macaca mulatta* Gal-10 induce agglutination of chicken erythrocytes. (B) *Macaca fascicularis* Gal-10 and *Macaca mulatta* Gal-10 induce agglutination of chicken erythrocytes that can be inhibited by lactose, with lactose having no effect on human Gal-10. (C) Sucrose could not inhibit hemagglutination induced by all three Gal-10s.

In Gal-10 from humans, *M. fascicularis* and *M. mulatta*, Tyr69, Phe69 and Phe72, respectively, are critical hotspots for crystal packing, with their aromatic side chains from two homodimers stacking in crystal-packing contacts (Figure 5). In our human Gal-10 dimer structure, electron density maps show that the two Tyr69 residues do not exhibit normal conformations, with their phenyl rings being so close as to appear to be covalently linked (Supplementary Figure S3). In addition, symmetry-related Tyr69 residues are concentrated within the lattice planes defined by the a and b axes of the unit cell and project outwards toward the edges of the human CLC lattice. This is why antibody binding to the region around Tyr69 effectively disrupts human CLCs [14].

Based on the above observations, we hypothesized that the free amino acids glycine, proline, cysteine, tyrosine, tryptophan, and phenylalanine may influence the aromatic ring stacking of Tyr69 residues. However, even 50 mM of these amino acids could not disrupt CLCs. Moreover, none of 50 mM urea, Triton X-100, Tween 20, NP-40 and common reducing agents DTT and β-mercaptoethanol had any effect on CLC formation. In contrast, NaOH effectively dissolved CLCs, which is consistent with previous studies [52].

Unlike DTT and β-mercaptoethanol, however, we discovered that reduced glutathione could effectively disrupt human CLCs (Figure 6 and Table 1). Reduced glutathione (12.5 mM) dissolved human CLCs in less than 92 s (Table 1). On the other hand, glutathione does not dissolve CLCs formed by monkey Gal-10 (Table 1). This indicates that the intrinsic characteristics of human and monkey CLCs are different. When we compared the primary and tertiary structures of these three Gal-10s, we found that Cys57 in human Gal-10 is located at a position analogous to that of Tyr57 and Tyr60 in the two monkey Gal-10s (Figure 5). Therefore, we tested the effects of glutathione on CLCs formed by the human Gal-10 C57A variant. After 6 hours of incubation, glutathione could not dissolve CLCs. This means that glutathione disrupts CLCs via its Cys57

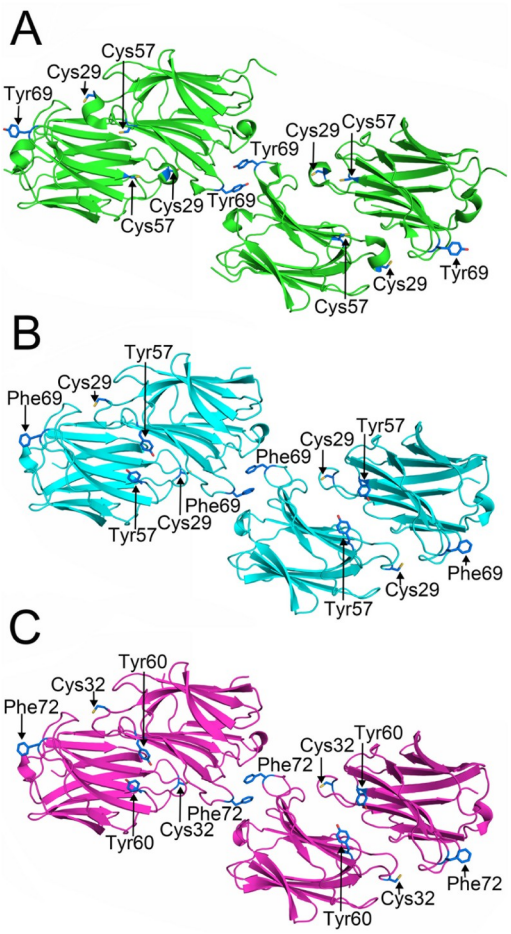

Figure 5. Key residues at the crystal packing contacts and dimer interface (A) Tyr69, located at the crystal packing contact site, could directly drive human Gal-10 CLC formation [14]. Cys29 and Cys57 from one human Gal-10 monomer face interact with the S-face of the other monomer. (B,C) Phe69 and Phe72 of *Macaca fascicularis* Gal-10 and *Macaca mulatta* Gal-10 play the same role as Tyr69 in human Gal-10. These residues can also promote monkey Gal-10 crystallization. Both *Macaca fascicularis* and *Macaca mulatta* Gal-10 have a conserved cysteine similar to human Gal-10 Cys29. However, there is a tyrosine residue in *Macaca fascicularis* Gal-10 and *Macaca mulatta* Gal-10, whereas human Gal-10 has Cys57.

residue, which is part of the ligand binding site on the CRD S-face. We hypothesized that glutathione might in fact influence the crystal-packing contact regions or change the global conformation of human Gal-10 by chemically modifying Cys57 to disrupt CLC formation. In addition, human Gal-10 contains another cysteine (Cys29) that is positioned not far from the ligand binding site outside the loop connecting the S5 and S6 β-strands. We found that glutathione disrupts CLCs formed with the C29A variant.

To better understand how CLCs are disrupted, we performed a CLC formation inhibition assay and found that 3 mM reduced glutathione effectively inhibits crystallization of human Gal-10. This suggests that it is easier for reduced glutathione to inhibit Gal-10 crystallization than to disrupt the already formed CLCs that require 12.5 mM GSH, an observation that is physiologically significant. In the cytoplasm, the concentration of reduced glutathione can reach 11 mM [53] and thus can inhibit Gal-10-mediated CLC formation. When Gal-10 is transported into the extracellular region where glutathione is normally in its oxidized state, Gal-10 quickly crystallizes. In addition, even 50 mM GSH does not inhibit crystallization of human Gal-10 C57A, monkey Gal-10 M1 or monkey Gal-10 M2 (Table 2). This supports our conclusion that GSH inhibits crystallization of human Gal-10 by chemically modifying Cys57.

Interaction between Gal-10 and tubulin α-1B.

To further understand the intracellular function of Gal-10, we employed pull-down experiments and mass spectrometry (MS) to identify protein partners with Gal-10. Here, we incubated HeLa cell lysates with His-Gal-10 and pulled down any Gal-10-binding partners using Ni-NTA beads, followed by SDS-PAGE and Coomassie blue staining (Figure 7A). The results show that Gal-10 indeed interacts with some HeLa cell-extracted protein(s) that we could identify by MS analysis of extracted SDS-PAGE bands. Several proteins, including tubulin α-1B and putative elongation factor 1-α-like 3, were identified by Nano-LC-ESI-MS/MS (Supplementary Table S2). MS parameters indicated that the band is most likely tubulin α-1B, a subtype of α-tubulin. Tubulin is found in all eukaryotic cells and is present in multiple isoforms. In mammals, there are at least six forms of α-tubulin, along with a similar number of β-tubulins, each encoded by a different gene. These forms of tubulin are very similar, and they generally copolymerize into

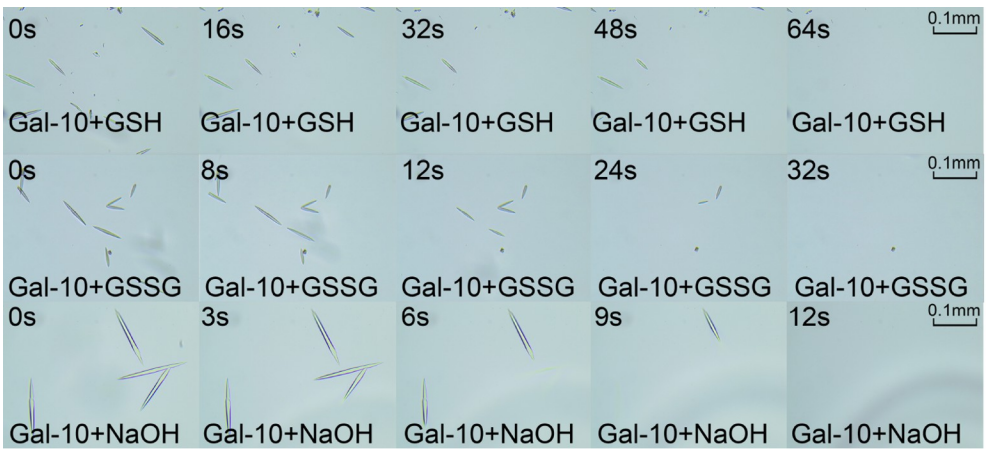

Figure 6. Time course assay of GSH, GSSG, and NaOH on the formation of human CLCs 25 mM GSH, 25 mM GSSG, and 25 mM NaOH effectively dissolved human CLCs.

Table 1. CLC dissolution assay

	3.125 mM (A/B/C)	6.25 mM (A/B/C)	12.5 mM (A/B/C)	25 mM (A/B/C)	50 mM (A/B/C)
Gal-10	(*/*/*)	(*/*/*)	(92s/56s/35s)	(64s/32s/12s)	(22s/22s/10s)
Gal-10 C29A	(*/*/*)	(*/*/*)	(18s/136s/*)	(16s/96s/75s)	(6s/64s/47s)
Gal-10 C57A	(*/*/*)	(*/*/*)	(*/*/*)	(*/*/*)	(*/*/*)
Macaca fascicularis Gal-10	(*/–/–)	(*/–/–)	(*/–/–)	(*/–/–)	(*/–/–)
Macaca mulatta Gal-10	(*/–/–)	(*/–/–)	(*/–/–)	(*/–/–)	(*/–/–)

A = reduced glutathione, B = oxidized glutathione, C = NaOH.

"*" means the compounds could not dissolve the proteins within 6 hours.

"–" means the effects were not determined.

Table 2. Inhibition of Gal-10 crystallization assay

	The lowest concentration of glutathione that can inhibit protein crystallization
Gal-10	3 mM
Gal-10 C29A	3 mM
Gal-10 C57A	*
Macaca fascicularis Gal-10	*
Macaca mulatta Gal-10	*

"*" means that 50 mM GSH could not inhibit human Gal-10 C57A, monkey Gal-10 M1 and M2 crystallization.

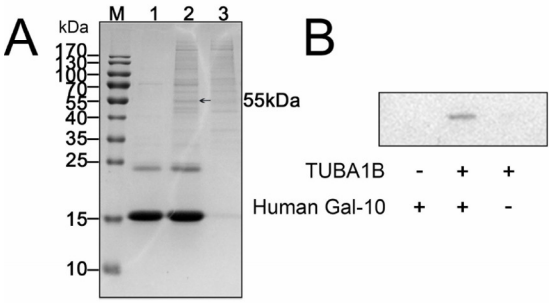

Figure 7. Determination of the interactions between Gal-10 and tubulin α-1B (A) His-tagged Gal-10 can specifically recover a protein from HeLa cell lysates. After SDS-PAGE, the protein band (indicated by an arrow) was cut from the gel and subject to MS analysis, which showed that the greatest possibility for the Gal-10 binding protein was tubulin α-1B. (B) His-tagged Gal-10 was incubated with HeLa cell lysates and pulled down with Ni-NTA beads, followed by western blotting analysis with antibodies against tubulin α-1B. TUBA1B: tubulin α-1B

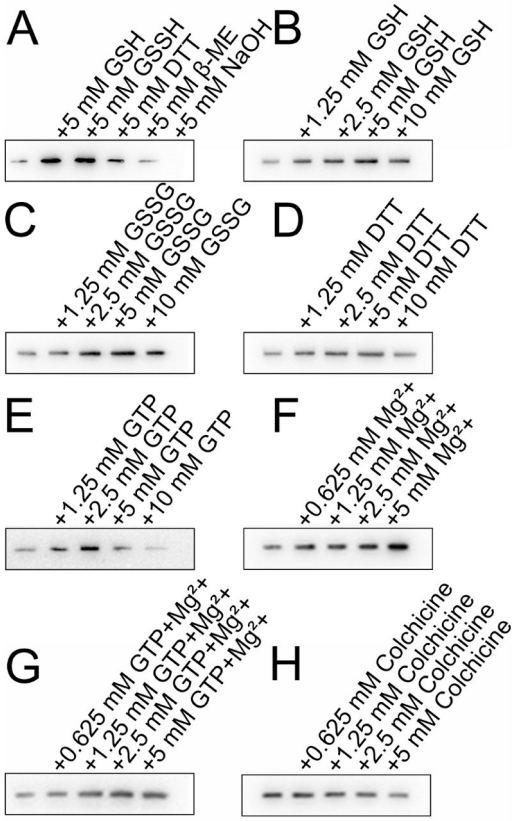

Figure 8. Effects of various compounds on the binding between Gal-10 and tubulin α-1B (A) GSH, GSSG and DTT (5 mM) stabilize the interaction between Gal-10 and tubulin α-1B, whereas β-mercaptoethanol cannot. (B– D) Concentration gradient assays of the effects of GSH, GSSG and DTT on the interaction between Gal-10 and tubulin α-1B. (E–H) Effects of GTP, Mg^{2+}, GTP + Mg^{2+} and colchicine on the interaction between Gal-10 and tubulin α-1B. The presence of GTP, Mg^{2+}, and GTP + Mg^{2+} enhances the binding between Gal-10 and tubulin α-1B. However, as the concentration of colchicine increases, colchicine tends to inhibit the binding between Gal-10 and tubulin α-1B.

mixed microtubules *in vitro*. In cells and tissues, microtubules are found at distinct locations with subtly different functions [54].

Using anti-tubulin α-1B antibodies and western blot analysis, we validated the binding between Gal-10 and tubulin α-1B (Figure 7B). Whereas this experiment showed that Gal-10 indeed binds to tubulin α-1B, tubulin α-1B in HeLa cell extracts (negative control) could not bind to Ni-NTA beads, indicating that binding between Gal-10 and tubulin α-1B is specific.

In the CLC disruption assay, we examined whether several compounds (*i.e.*, GSH, GSSG, DTT, β-mercaptoethanol and NaOH) could modulate the interactions between Gal-10 and tubulin α-1B. Our results show that GSH and GSSG significantly improve the binding between Gal-10 and tubulin α-1B, disrupt CLCs, and inhibit Gal-10 crystallization (Figure 8A). On the other hand, DTT only slightly increased the binding between Gal-10 and tubulin α-1B, whereas β-mercaptoethanol had no effect, and NaOH completely inhibited this binding, possibly by somehow modifying the overall fold of either or both proteins (Figure 8A).

Subsequently, we examined the concentration dependence of GSH, GSSG and DTT on Gal-10/ tubulin α-1B binding. At 5 mM, these compounds increased Gal-10/ tubulin α-1B binding the most (Figure 8B–D). In the CLC disruption assay, GSH and GSSG were most effective, supporting the idea that both compounds can modify the global conformation of Gal-10 and/or stabilize the structure of

tubulin α-1B to enhance intermolecular interactions. Although DTT is also a reducing agent similar to GSH, it had no effect on Gal-10.

We also investigated the effects of GTP, Mg^{2+} and colchicine on Gal-10/ tubulin α-1B binding. Microtubules are polymers of tubulin heterodimers composed of GTP-bound α- and β-tubulin molecules that associate laterally to form hollow microtubules. The GTP-Mg^{2+} that is bound to α-tubulin is physically trapped at the dimer interface and is not hydrolyzed or exchanged and, as such, is an integral part of the tubulin heterodimer structure. Colchicine can bind to soluble tubulin to form tubulin-colchicine complexes. At low concentrations, colchicine arrests microtubule growth, but at higher concentrations, it promotes microtubule depolymerization [55]. Here, we found that GTP and Mg^{2+} increase the binding between Gal-10 and tubulin α-1B (Figure 8). In contrast, the presence of colchicine in the pull-down buffer slightly inhibits the interaction between Gal-10 and tubulin α-1B, implying that colchicine binding to tubulin α-1B and/or colchicine-induced microtubule disruption attenuate the binding between Gal-10 and tubulin α-1B.

Discussion

In 1872, Ernst Viktor von Leyden described the colorless CLCs found in the sputum of asthma patients [2]. Later studies showed that CLCs are present in the respiratory tracts of asthmatic patients [14,56]. Recently, mouse experiments showed that CLCs can directly cause asthma [14], and in a humanized mouse model of asthma, anti-CLC antibodies disrupted CLCs and reversed crystal-driven inflammation, goblet-cell metaplasia, immunoglobulin E (IgE) synthesis, and bronchial hyperreactivity (BHR) [14]. Here, we found that GSH also disrupts CLCs and inhibits CLC formation. In fact, GSH is the most abundant antioxidant found in the epithelial lining fluid of airways, with concentrations ∼140-fold higher (approximately 429 μM) than that observed in plasma (approximately 3 μM) [57]. In addition, GSH can also significantly delay apoptosis in sodium arsenite-stimulated or -unstimulated eosinophils [58]. Even though 1 mM GSH was used in that study, we thought that approximately half that concentration (*i.e.*, 429 μM) could be effective. If the lower concentration of GSH in eosinophilic asthma patient airways does not prevent eosinophil apoptosis, Gal-10 release may induce CLC formation and promote asthma.

In addition, GSH is the predominant intracellular thiol, and GSSG concentrations are typically very low. Inside the cell, CLC formation is dependent on the GSH concentration, which ranges from 1 to 11 mM [53]. However, at 3 mM, GSH inhibits CLC formation, whereas at lower concentrations, it does not. The fact that the concentration of GSH in the cytoplasm fluctuates may help explain why Gal-10 sometimes forms CLCs in the cytoplasm and at other times does not. The concentrations of GSH and GSSG outside the cell are usually 100 to 1000 times less than those inside the cell [59], leading to spontaneous formation of CLCs when Gal-10 is released from eosinophils [9,15,22]. The GSH concentration in that environment is likely to be too low to inhibit CLC formation. Therefore, GSH has a dual function by inhibiting both eosinophil apoptosis and CLC formation. Both GSH-mediated events can relieve asthmatic symptoms.

Because GSH is already available on the market, further investigation as to whether GSH can be used to treat eosinophilic diseases, such as asthma, is warranted, with animal experiments likely leading the way. The Gal-10 gene is only present in primates [35,60], and in biomedical research, *M. fascicularis* and *M. mulatta* are widely used monkey models [61,62]. In both species, the Gal-10 gene is present with only a few amino acid variations in their ligand binding sites (Tyr57/60 and Glu75/78, respectively) compared to those of human Gal-10 (Cys57 and Gln75). Moreover, our crystal structures and hemagglutination assays demonstrate that these monkey Gal-10s can bind to lactose, whereas human Gal-10 cannot, indicating that lactose binding to human Gal-10 is not crucial for its primary physiological function. During evolution, the human Gal-10 gene encoding tyrosine (TAC) and glutamate (GAG) was mutated to cysteine (TGC) and glutamine (CAG), respectively, causing human Gal-10 to lose its ability to bind to lactose or galactose. Most importantly, human CLCs can be applied directly in the airways of these monkeys to assess the effects of GSH on CLCs because their CLCs are insensitive to GSH or GSSG. Alternatively, one could knock out the Gal-10 gene in monkeys and knock in the human Gal-10 gene to assess the effect of GSH on CLCs. Overall, our present study supports the idea of using these models to explore the effect of GSH on CLC formation.

Gal-10 is also found in the outer cell membrane of T cells, where it can suppress T-cell function [37]. Previous studies with human peripheral eosinophils have demonstrated that there is a large amount of Gal-10 in the nucleus [16,63]. Our previous work with Gal-10 indicated that EGFP-tagged lectin is primarily distributed in the nucleus of HeLa cells [25]. Other reports have shown that Gal-10 is also located in the cytoplasm [17,36,64]. However, a recent study showed that Gal-10 is not stored in granules but rather resides in the peripheral cytoplasm of human eosinophils [38].

Although the distribution of Gal-10 in cells has been extensively investigated, the function of Gal-10 in cells remains unknown or unclear. To date, only two enzymes have been found to bind to Gal-10, i.e., lysophospholipase [23] and eosinophil granule cationic RNases [eosinophil-derived neurotoxin (RNS2), as well as eosinophil cationic protein (RNS3)]. These proteins arise during cell differentiation and degranulation to enable intracellular packaging and extracellular allergic inflammation [39]. Here, we discovered that Gal-10 also binds to tubulin α-1B, an abundant protein within the cell. Therefore, we hypothesized that this interaction may regulate the distribution or secretion of Gal-10 via its binding to tubulin. However, the details of this interaction require further investigation.

In summary, we discovered that GSH, a common reducing agent in the human body, disrupts CLCs and inhibits Gal-10 crystallization. As a pharmaceutical drug, GSH has the potential to combat eosinophilic-based diseases induced by CLCs. We also found that Gal-10 from *M. fascicularis* and *M. mulatta* promoted CLC formation. The crystal structures of both Gal-10s show that they can bind to lactose, unlike human Gal-10, due to an evolutionary mutation of two key lactose binding residues (positions 57 and 75). Finally, we identified tubulin α-1B as a new binding partner for Gal-10. Overall, our study suggests that GSH may be used to better understand Gal-10 function and the formation of CLCs. This, in turn, suggests that GSH may be used as a pharmaceutical agent to ameliorate CLC-induced diseases.

Supplementary Data

Supplementary data is available at *Acta Biochimica et Biophysica Sinica* online.

Acknowledgement

We are very grateful to the staffs of the BL17B/BL18U/BL19U1/BL19U2/BL01B beamline at the Shanghai Synchrotron Radiation Facility of the National Facility for Protein Science Shanghai (NFPS) for their assistance in data collection.

Funding

This work was supported by the grants from the National Natural Science Foundation of China (No. 32171255) and Industrialization Cultivation Planning Project of Jilin Provincial Department of Education (No. JJKH20221168CY).

Conflict of Interest

The authors declare that they have no conflict of interest.

References

1. Charcot JM, Robin C. Observation de leucocythemie. *C R Seances Mem Soc Biol* 1853, 5: 44–52
2. Leyden E. Zur Kenntniss des bronchial asthma. *Archiv für pathologische Anatomie und Physiologie und für klinische Medicin* 1872, 54: 324–344
3. Leffler H, Masiarz FR, Barondes SH. Soluble lactose-binding vertebrate lectins: a growing family. *Biochemistry* 1989, 28: 9222–9229
4. Ackerman SJ, Corrette SE, Rosenberg HF, Bennett JC, Mastrianni DM, Nicholson-Weller A, Weller PF, *et al.* Molecular cloning and characterization of human eosinophil Charcot-Leyden crystal protein (lysophospholipase). Similarities to IgE binding proteins and the S-type animal lectin superfamily. *J Immunol* 1993, 150: 456–468
5. Barondes SH, Cooper DN, Gitt MA, Leffler H. Galectins. Structure and function of a large family of animal lectins. *J Biol Chem* 1994, 269: 20807–20810
6. Leffler H, Carlsson S, Hedlund M, Qian Y, Poirier F. Introduction to galectins. *Glycoconj J* 2002, 19: 433–440
7. Acharya KR, Ackerman SJ. Eosinophil granule proteins: form and function. *J Biol Chem* 2014, 289: 17406–17415
8. Dvorak AM, Letourneau L, Login GR, Weller PF, Ackerman SJ. Ultrastructural localization of the Charcot-Leyden crystal protein (lysophospholipase) to a distinct crystalloid-free granule population in mature human eosinophils. *Blood* 1988, 72: 150–158
9. Ayres WW. Production of Charcot-Leyden crystals from eosinophils with aerosol MA. *Blood* 1949, 4: 595–602
10. Lao LM, Kumakiri M, Nakagawa K, Ishida H, Ishiguro K, Yanagihara M, Ueda K. The ultrastructural findings of Charcot-Leyden crystals in stroma of mastocytoma. *J Dermatological Sci* 1998, 17: 198–204
11. Bryborn M, Halldén C, Säll T, Cardell LO. CLC– a novel susceptibility gene for allergic rhinitis? *Allergy* 2010, 65: 220–228
12. De Re V, Simula MP, Cannizzaro R, Pavan A, de Zorzi MA, Toffoli G, Canzonieri V. Galectin-10, eosinophils, and celiac disease. *Ann New York Acad Sci* 2009, 1173: 357–364
13. Staribratova D, Belovejdov V, Staikov D, Dikov D. Demonstration of Charcot-Leyden crystals in eosinophilic cystitis. *Arch Pathol Laboratory Med* 2010, 134: 1420
14. Persson EK, Verstraete K, Heyndrickx I, Gevaert E, Aegerter H, Percier JM, Deswarte K, *et al.* Protein crystallization promotes type 2 immunity and is reversible by antibody treatment. *Science* 2019, 364: eaaw4295
15. Samter M. Charcot-Leyden crystals, a study of the conditions necessary for their information. *J Allergy* 1947, 18: 221–230
16. Zhou Z, Teneri DG, Dvorak AM, Ackerman SJ. The gene for human eosinophil Charcot-Leyden crystal protein directs expression of lysophospholipase activity and spontaneous crystallization in transiently transfected COS cells. *J Leukocyte Biol* 1992, 52: 588–595
17. Dvorak AM, Furitsu T, Letourneau L, Ishizaka T, Ackerman SJ. Mature eosinophils stimulated to develop in human cord blood mononuclear cell cultures supplemented with recombinant human interleukin-5. Part I. Piecemeal degranulation of specific granules and distribution of Charcot-Leyden crystal protein. *Am J Pathol* 1991, 138: 69–82
18. Yang RY, Rabinovich GA, Liu FT. Galectins: structure, function and therapeutic potential. *Expert Rev Mol Med* 2008, 10: e17
19. Kasai K, Hirabayashi J. Galectins: a family of animal lectins that decipher glycocodes. *J Biochem* 1996, 119: 1–8
20. Cooper DN. Galectinomics: finding themes in complexity. *Biochim Biophys Acta Gen Subj* 2002, 1572: 209–231
21. Leonidas DD, Elbert BL, Zhou Z, Leffler H, Ackerman SJ, Acharya KR. Crystal structure of human Charcot–Leyden crystal protein, an eosinophil lysophospholipase, identifies it as a new member of the carbohydrate-binding family of galectins. *Structure* 1995, 3: 1379–1393
22. Swaminathan GJ, Leonidas DD, Savage MP, Ackerman SJ, Acharya KR. Selective recognition of mannose by the human eosinophil Charcot-Leyden crystal protein (galectin-10): a crystallographic sudy at 1.8 Å resolution. *Biochemistry* 1999, 38: 13837–13843
23. Ackerman SJ, Liu L, Kwatia MA, Savage MP, Leonidas DD, Swaminathan GJ, Acharya KR. Charcot-Leyden crystal protein (galectin-10) is not a dual function galectin with lysophospholipase activity but binds a lysophospholipase inhibitor in a novel structural fashion. *J Biol Chem* 2002, 277: 14859–14868
24. Itoh A, Nonaka Y, Nakakita S, Yoshida H, Nishi N, Nakamura T, Kamitori S. Structures of human galectin-10/monosaccharide complexes demonstrate potential of monosaccharides as effectors in forming Charcot-Leyden crystals. *Biochem Biophys Res Commun* 2020, 525: 87–93
25. Su J, Gao J, Si Y, Cui L, Song C, Wang Y, Wu R, *et al.* Galectin-10: a new structural type of prototype galectin dimer and effects on saccharide ligand binding. *Glycobiology* 2018, 28: 159–168
26. Su J, Song C, Si Y, Cui L, Yang T, Li Y, Wang H, *et al.* Identification of key amino acid residues determining ligand binding specificity, homodimerization and cellular distribution of human galectin-10. *Glycobiology* 2019, 29: 85–93
27. López-Lucendo MF, Solís D, Andre S, Hirabayashi J, Kasai Ki, Kaltner H, Gabius HJ, *et al.* Growth-regulatory human galectin-1: crystallographic characterisation of the structural changes induced by single-site mutations and their impact on the thermodynamics of ligand binding. *J Mol Biol* 2004, 343 4: 957–970
28. Si Y, Feng S, Gao J, Wang Y, Zhang Z, Meng Y, Zhou Y, *et al.* Human galectin-2 interacts with carbohydrates and peptides non-classically: new insight from X-ray crystallography and hemagglutination. *Acta Biochim Biophys Sin* 2016, 48: 939–947
29. Leonidas DD, Vatzaki EH, Vorum H, Celis JE, Madsen P, Acharya KR. Structural basis for the recognition of carbohydrates by human galectin-7. *Biochemistry* 1998, 37: 13930–13940
30. Su J, Wang Y, Si Y, Gao J, Song C, Cui L, Wu R, *et al.* Galectin-13, a different prototype galectin, does not bind β-galacto-sides and forms dimers via intermolecular disulfide bridges between Cys-136 and Cys-138. *Sci Rep* 2018, 8: 980
31. Yang T, Yao Y, Wang X, Li Y, Si Y, Li X, Ayala GJ, *et al.* Galectin-13/placental protein 13: redox-active disulfides as switches for regulating structure, function and cellular distribution. *Glycobiology* 2020, 30: 120–129
32. Li X, Yao Y, Liu T, Gu K, Han Q, Zhang W, Ayala GJ, *et al.* Actin binding to galectin-13/placental protein-13 occurs independently of the galectin canonical ligand-binding site. *Glycobiology* 2021, 31: 1219–1229

33. Si Y, Li Y, Yang T, Li X, Ayala GJ, Mayo KH, Tai G, *et al.* Structure-function studies of galectin-14, an important effector molecule in embryology. *FEBS J* 2021, 288: 1041–1055
34. Si Y, Yao Y, Jaramillo Ayala G, Li X, Han Q, Zhang W, Xu X, *et al.* Human galectin-16 has a pseudo ligand binding site and plays a role in regulating c-Rel-mediated lymphocyte activity. *Biochim Biophys Acta Gen Subj* 2021, 1865: 129755
35. Su J. A brief history of charcot-leyden crystal protein/galectin-10 research. *Molecules* 2018, 23: 2931
36. Dvorak AM, Macglashan DW, Warner JA, Letourneau L, Morgan ES, Lichtenstein LM, Ackerman SJ. Localization of Charcot-Leyden crystal protein in individual morphological phenotypes of human basophils stimulated by f-Met peptide. *Clin Exp Allergy* 1997, 27: 452–474
37. Kubach J, Lutter P, Bopp T, Stoll S, Becker C, Huter E, Richter C, *et al.* Human CD4 + CD25 + regulatory T cells: proteome analysis identifies galectin-10 as a novel marker essential for their anergy and suppressive function. *Blood* 2007, 110: 1550–1558
38. Melo RCN, Wang H, Silva TP, Imoto Y, Fujieda S, Fukuchi M, Miyabe Y, *et al.* Galectin-10, the protein that forms Charcot-Leyden crystals, is not stored in granules but resides in the peripheral cytoplasm of human eosinophils. *J Leukocyte Biol* 2020, 108: 139–149
39. Grozdanovic MM, Doyle CB, Liu L, Maybruck BT, Kwatia MA, Thiyagarajan N, Acharya KR, *et al.* Charcot-Leyden crystal protein/galectin-10 interacts with cationic ribonucleases and is required for eosinophil granulogenesis. *J Allergy Clin Immunol* 2020, 146: 377–389
40. Kabsch W. *XDS*. *Acta Crystlogr D Biol Crystlogr* 2010, 66: 125–132
41. Battye TGG, Kontogiannis L, Johnson O, Powell HR, Leslie AGW. *iMOSFLM*: a new graphical interface for diffraction-image processing with *MOSFLM*. *Acta Crystlogr D Biol Crystlogr* 2011, 67: 271–281
42. Sanz-Gaitero M, Keary R, Garcia-Doval C, Coffey A, van Raaij MJ. Crystallization of the CHAP domain of the endolysin from *Staphylococcus aureus* bacteriophage K. *Acta Crystlogr F Struct Biol Cryst Commun* 2013, 69: 1393–1396
43. Potterton E, Briggs P, Turkenburg M, Dodson E. A graphical user interface to the *CCP* 4 program suite. *Acta Crystlogr D Biol Crystlogr* 2003, 59: 1131–1137
44. McCoy AJ. Solving structures of protein complexes by molecular replacement with *Phaser*. *Acta Crystlogr D Biol Crystlogr* 2007, 63: 32–41
45. Adams PD, Afonine PV, Bunkóczi G, Chen VB, Davis IW, Echols N, Headd JJ, *et al.* *PHENIX*: a comprehensive Python-based system for macromolecular structure solution. *Acta Crystlogr D Biol Crystlogr* 2010, 66: 213–221
46. Davis IW, Leaver-Fay A, Chen VB, Block JN, Kapral GJ, Wang X, Murray LW, *et al.* MolProbity: all-atom contacts and structure validation for proteins and nucleic acids. *Nucleic Acids Res* 2007, 35: W375–W383
47. Chen VB, Arendall Iii WB, Headd JJ, Keedy DA, Immormino RM, Kapral GJ, Murray LW, *et al.* *MolProbity*: all-atom structure validation for macromolecular crystallography. *Acta Crystlogr D Biol Crystlogr* 2010, 66: 12–21
48. Pettersen EF, Goddard TD, Huang CC, Couch GS, Greenblatt DM, Meng EC, Ferrin TE. UCSF Chimera? A visualization system for exploratory research and analysis. *J Comput Chem* 2004, 25: 1605–1612
49. Su J, Cui L, Si Y, Song C, Li Y, Yang T, Wang H, *et al.* Resetting the ligand binding site of placental protein 13/galectin-13 recovers its ability to bind lactose. *Biosci Rep* 2018, 38
50. Su J, Zhang T, Wang P, Liu F, Tai G, Zhou Y. The water network in galectin-3 ligand binding site guides inhibitor design. *Acta Biochim Biophys Sin* 2015, 47: 192–198
51. Si Y, Wang Y, Gao J, Song C, Feng S, Zhou Y, Tai G, *et al.* Crystallization of galectin-8 linker reveals intricate relationship between the N-terminal tail and the linker. *Int J Mol Sci* 2016, 17: 2088
52. Bai XL. A case report of acute promyelocytic leukemia with increased granulation with Charcot-Leyden crystals. *Qinghai Medical Journal* 1998, 5: 56
53. Smith CV, Jones DP, Guenthner TM, Lash LH, Lauterburg BH. Compartmentation of glutathione: implications for the study of toxicity and disease. *Toxicol Appl Pharmacol* 1996, 140: 1–12
54. Alberts B, Johnson A, Lewis J, Morgan D, Raff M, Roberts K, Walter P, Wilson J, Hunt T. Molecular Biology of the Cell, 6nd Ed.W.W. Norton & Company, New York 2015
55. Leung YY, Yao Hui LL, Kraus VB. Colchicine—update on mechanisms of action and therapeutic uses. *Semin Arthritis Rheumatism* 2014, 45: 341–350
56. Welsh RA. The genesis of the Charcot-Leyden crystal in the eosinophilic leukocyte of man. *Am J Pathol* 1959, 35: 1091–1103
57. Cantin AM, North SL, Hubbard RC, Crystal RG. Normal alveolar epithelial lining fluid contains high levels of glutathione. *J Appl Physiol* 1987, 63: 152–157
58. Wedi B, Straede J, Wieland B, Kapp A. Eosinophil apoptosis is mediated by stimulators of cellular oxidative metabolisms and inhibited by antioxidants: involvement of a thiol-sensitive redox regulation in eosinophil cell death. *Blood* 1999, 94: 2365–2373
59. Schafer FQ, Buettner GR. Redox environment of the cell as viewed through the redox state of the glutathione disulfide/glutathione couple. *Free Radical Biol Med* 2001, 30: 1191–1212
60. Mastrianni DM, Eddy RL, Rosenberg HF, Corrette SE, Shows TB, Tenen DG, Ackerman SJ. Localization of the human eosinophil Charcot-Leyden crystal protein (Lysophospholipase) gene (CLC) to chromosome 19 and the human ribonuclease 2 (eosinophil-derived neurotoxin) and ribonuclease 3 (eosinophil cationic protein) genes (RNS2 and RNS3) to chromosome 14. *Genomics* 1992, 13: 240–242
61. Bolton ID. Chapter 5-Basic Physiology of Macaca fascicularis. In: Bluemel J, Korte S, Schenck E, Weinbauer GF eds. *The Nonhuman Primate in Nonclinical Drug Development and Safety Assessment* San Diego: Academic Press 2015: 67–86
62. Beran MJ, Evans TA, Klein ED, Einstein GO. Rhesus monkeys (Macaca mulatta) and capuchin monkeys (*Cebus apella*) remember future responses in a computerized task. *J Exp Psychol-anim Behav Processes* 2012, 38: 233–243
63. Calafat J, Janssen H, Knol EF, Weller PF, Egesten A. Ultrastructural localization of Charcot - Leyden crystal protein in human eosinophils and basophils. *Eur J Haematology* 1997, 58: 56–66
64. Gleich GJ, Loegering DA, Adolphson CR. Eosinophils and bronchial inflammation. *Chest* 1985, 87: 10S–13S